ADVANCED FUNCTIONAL MATERIALS

FULL PAPER

DOI: 10.1002/adfm.200600731

Blue Electroluminescence Enhancement of Poly{2,7-(9,9′-dioctylfluorene)-*co*-4-diphenylamino-4′-bipenylmethylsulfide} Incorporating Side-Chain-Tethered Gold Nanoparticles**

By *So-Lin Hsu*, *Chia-Hung Chou*, *Chen-Ping Chen*, and *Kung-Hwa Wei**

Through in situ reduction of a gold precursor, we have tethered gold nanoparticles (Au NPs) to the side chains of poly{2,7-(9,9′-dioctylfluorene)-*co*-4-diphenylamino-4′-bipenylmethylsulfide} (PF-DBMS) through its $ArSCH_3$ anchor groups. The presence of 1 wt % of the tethered Au NPs led to a reduction in the degree of aggregation of the polymer chains, resulting in a 50 % increase in its quantum yield. The electroluminescence of a 1 wt % Au/PF-DBMS device was almost four times higher in terms of its maximum brightness and its full-width-at-half-maximum emission peak was much narrower than that of a pure PF-DBMS device; the presence of a small amount of Au NPs significantly enhances the electron injection and transport and suppresses the photo-oxidation of PF-DBMS.

1. Introduction

Conjugated polymer/nanoparticles nanocomposites have great potential for application in flexible optical and electronic devices[1,2] because (a) modifying the molecular structure of the polymer and its solution processing are both relatively easy tasks and (b) colloidal nanoparticles can be fabricated with adjustable surface ligands for solution processing. Depending upon the type of material sought, three approaches are typically used to prepare these composites: in situ synthesis of nanoparticles in a polymer matrix,[3] mixing polymers and nanoparticles in solvents,[4,5] and in situ polymerization of monomers in the presence of nanoparticles.[6] In the cases of in situ polymerization of monomers, most of them have to be carried out in dilute solutions, resulting in limited quantity.[7] Composites made from mixing polymers and nanoparticles in solvents sometimes have nanoparticles aggregation and phase separation.[3a,b] Whereas, in situ synthesis[3c] of nanoparticles in the presence of polymer can be more challenging chemically but can reduces the dispersity and aggregation of nanoparticles, creating more homogeneous composites.[3e,f] In this study, we chose polyfluorene copolymer and in situ synthesized gold nanoparticles (Au NPs) to be the components of the material, with chemical bonding of the Au NPs occurring through the side chains of the polyfluorene copolymer by design. To the best of our knowledge, Au NPs have never previously been attached to the side chains of luminescent polymers.

Polyfluorene and its derivatives are among the best performing of the blue light emitting polymers,[8–10] but their device applications are limited by poor emission spectral stability and the development of undesired emissions of green light[11–13] arising from photo-oxidation of the carbon bridge or from aggregation of the polymer chains.[14] The tethering of CdS semiconductor NPs of various sizes to the side chains of a dendritic polyfluorene—through π–π stacking between the ligands on the NPs and the dendritic groups—appears to produce a bluer and brighter light relative to that of the pure dendritic polyfluorene.[15] Unfortunately, such π–π stacking in dendritic polyfluorene/NP hybrids can be sustained only at mild temperatures (ca. $<60\,^{\circ}C$) and at relatively semi-concentrated particle concentrations (ca. 8 %). Moreover, the toxicity of CdS NPs prevents them from being used as major components of the composites for environmental reasons. On the other hand, Au NPs, which are used in, for example, DNA detection and other studies involving surface-enhanced Raman scattering, are considered to be friendlier to the environment and to living creatures. A recent study found that blending Au NPs with polyfluorene resulted in enhanced luminescent stability.[16] The effect of the Au NPs appears to be limited because the uniform distribution of gold NPs in polyfluorene—in the absence of any specific interaction or bonding to the polymer—is very difficult to achieve. In this paper, we describe how the tethering of Au NPs to the side chains of a poly{2,7-(9,9′-dioctylfluorene)-*co*-4-diphenylamino-4′-bipenylmethylsulfide} (PF-DBMS), through chemical bonds, leads to enhanced electroluminescence with no detectable change in the emission wavelength of the polymer; the side-chain tethered Au NPs will not affect the conjugation length of the main chain. From using this approach, the tethered Au NPs appear to effectively prevent aggregation of

[*] Prof. K. H. Wei, S.-L. Hsu, C. H. Chou, C. P. Chen
Department of Materials Science and Engineering
National Chiao Tung University
1001 Ta Hsueh Road, Hsinchu 30050, Taiwan, ROC
E-mail: khwei@mail.nctu.edu.tw

[**] We acknowledge the National Science Council, Taiwan, for funding this work through grants NSC 94-2120M-009-001. We are grateful to Prof. Yao-Wing Yang, Dr. Siao-Wei Yeh, and Mr. Chin-Mao Huang for their experimental assistance and helpful discussions.

the PF-DBMS polymer chains while serving as facilitators for enhancing its thermal stability and suppressing the keto defect of the fluorene units, thereby not only increasing the quantum yield but also enhancing the EL performance of the devices. Scheme 1 provides a schematic illustration of this copolymer's molecular structure and how it incorporates the Au NPs. We synthesized poly{2,7-(9,9′-dioctylfluorene)-*co*-4-diphenylamino-4′-bipenylmethylsulfide}(PF-DBMS), dissolved it in toluene, and then added $HAuCl_4$—the precursor of the Au NPs—to the solution. Subsequently, $NaBH_4$ was added to reduce this precursor and form the Au NPs. The stability of Au NPs in various media is determined by the nature of their surface ligands, which are typically alkanethiols having various carbon chain lengths. Several groups have reported the chemisorption of alkane or polymer-terminated thiols onto the surfaces of gold NPs to form self-assembled monolayers. Other sulfur-containing ligands—such as disulfides (–S–S–),[17–20] thioethers ($–SCH_3$),[21] di-[22] and trithiols,[23] and resorcinarene tetrathiols[24]—can also be used to stabilize AuNPs, but their binding abilities are not as high as those of the alkanethiols. To compensate for the weaker interactions between AuNPs and thioethers, polymers containing multiple thioether units are required to produce stable and well-ordered monolayers from such systems.[25a] Because the use of end-grafting techniques to fix either thioether derivatives or polymer molecules onto the Au surfaces limits the number of NPs that can be bound to each chain, we prepared a series of polymers possessing multiple thioether bonding sites on their side chains (i.e., more bonding points per polymer molecule would be available for chemisorption, see Scheme 2). Thus, we brominated triphenylamine, reacted the tribromide with 4-(methylthio)benzeneboronic acid (Suzuki coupling), and then polymerized the dibromide/monothioether in the presence of fluorene monomers (Scheme 1).

2. Results and Discussion

The chemical structures of the products were determined using ^1H NMR spectroscopy (Fig. 1); in this paper, we use the acronym PF-DBMS to represent the copolymer containing a 10 % molar ratio of DBMS repeat units in the polyfluorene.

We used X-ray photoelectron spectroscopy (XPS) to confirm that chemical bonding occurred between the Au NPs and PF-DBMS (Fig. 2). Because of spin-orbit splitting,[25b] this spectrum exhibits two sets of doublets (S and S′) that reveal the binding energies of the bound and unbound sulfur species, respectively. Peak fitting revealed that the binding energies of unbound S′($2P_{3/2}$) and S′ ($2P_{1/2}$) were 163.3 and 164.2 eV, respectively, while the peak of bound S($2P_{3/2}$) and S($2P_{1/2}$) were centered at 161.7 and 162.4 eV, respectively.[25c,d] A reduction of 1.6 eV from S′ to S corresponds to the effect of sulfur atoms bound to the gold—direct evidence for bonding of the $ArSCH_3$ functional groups to the Au NPs. Figure 3 displays the UV-vis absorption and photoluminescence spectra of PF-DBMS. In THF, PF-DBMS displayed signal maxima at 387 and 427 nm for its ab-

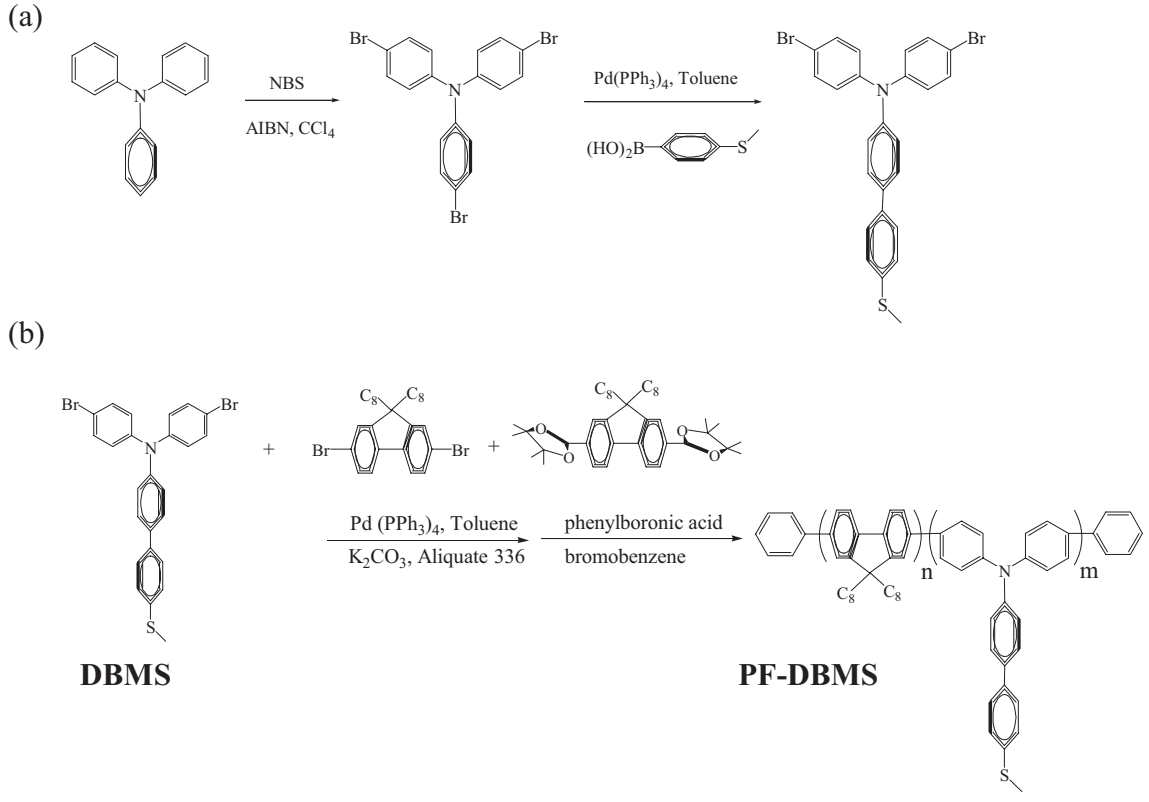

Scheme 1. Synthesis of a) DBMS and PF-DBMS copolymers b) A schematic drawing of the architecture of Au/PF-DBMS nanocomposites.

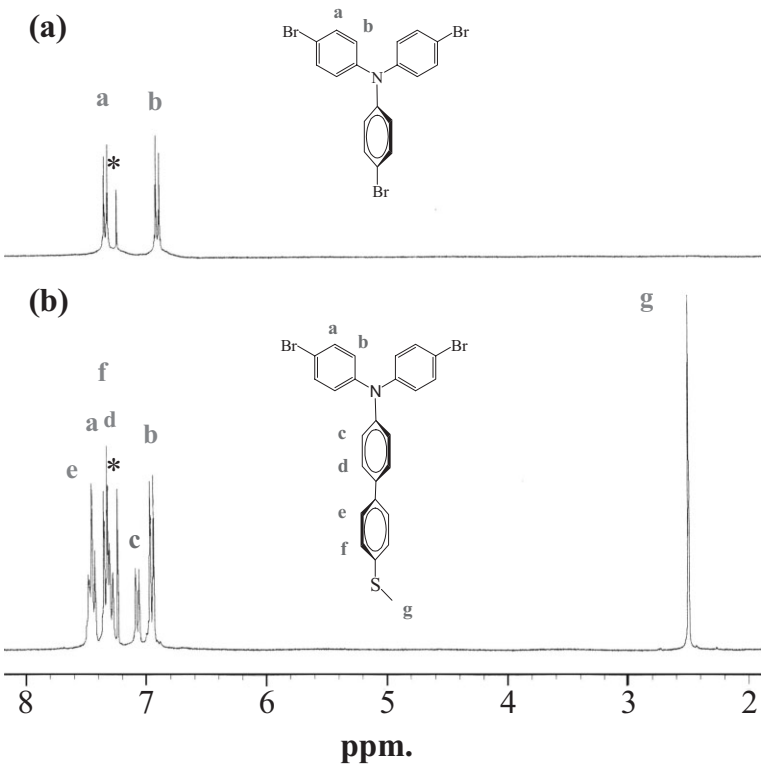

Figure 1. ^{1}H NMR spectra of a) tris(4-bromophenyl)amine and b) DBMS.

sorption and emission, respectively; the emission maximum shifted to 440 nm in the solid state. Moreover, the inset to Figure 3 clearly indicates an improved stability of the PL emission characteristics of the PF-DBMS/Au NP, relative to those of PF-DBMS, after thermal treatment of 100 °C for 2 h. This situation results from the number of triplet excitons, which are the major cause of oxidation of PF-DBMS, being reduced as a result of energy transfer from the triplet emission band of PF-DBMS[26–28] to the optical absorption bands of the Au NPs (ca. 520 nm). To obtain a quantitative assessment of the luminance of these composites, we used Beer's law to determine their quantum yields, which are listed in Table 1 along with the optical parameters of the composite films. Substantial improvements in the quantum yields of the composites occurred when a small weight percentage of Au NPs was present in the PF-DBMS. For instance, the quantum yield of PF-DBMS incorporating 1 wt % Au NPs improved to (0.86 ± 0.03) from (0.57 ± 0.02) for pure PF-DBMS—, i.e., a 50 % increase in quantum yield occurred upon adding the Au NPs. This increase in quantum yield in the presence of the Au NPs presumably results from reduced aggregation of the polymer chains upon their binding to the side-chain-tethered Au NPs. Figure 4 shows X-ray diffraction results of PF-DBMS/Au NP nanocomposites. The packing of PF-DBMS chains in the solid state was found to be amorphous by X-ray diffraction experiments, with two broad correlation peaks. The peak that remains at $2\theta = 20.5°$ (d-spacing = 4.3 Å), despite the variation in the amount of gold nanoparticles, is due to the average C–C intermolecular distance (i.e., the distance between the pendent group of the polymer chains) of PF-DBMS, while the other peak at lower diffraction angle, $2\theta = 3$–$5°$ that changes with the amount gold nanoparticles is a measurement of the average inter polymer chain distance.[12d,28b] As the amount of NPs increases to 6 % in PF-DBMS, the interchain distance peak shifted from $2\theta = 4.8°$ (18.4 Å) to an diffraction angle, $2\theta = 3.6°$ (24.5 Å), suggesting that the polymer chains are further apart and a disordering of polymer chains could have happened. However, when we increased the concentration of Au NPs in PF-DBMS to 6 wt %, the quantum yield of this composite decreased to (0.54 ± 0.03). This phenomenon resulted from the Au NPs also absorbing singlet exciton energy. Thus, we found that the optimal quantum yield occurred for the composite containing 1 wt % Au NPs in PF-DBMS. We determined the degree of dispersion of the Au NPs in PF-DBMS from transmission electron microscopy (TEM) images of the PF-DBMS/Au NP composites; Figure 5a indicates that the distribution of Au NPs ((3.8 ± 0.3) nm in diameter) was uniform in terms of both their thickness and across a cross-sectional cut-away view. Figure 5b displays a histogram of the size distribution of the NPs. Figure 5c provides a cross-sectional view of the PF-DBMS/Au device used for the electroluminescence study; it appears that the dispersion of Au NPs in PF-DBMS is rather homogeneous and some of the Au NPs were located close to the interface of the electrode.

Figure 7a displays the current–voltage characteristics of PF-DBMS and the PF-DBMS/Au NP device. The most interesting phenomenon we observe is the dramatic increase in current that occurred when 0.5 wt % Au NPs were incorporated into the PF-DBMS, suggesting that the presence of the Au NPs in PF-DBMS enhances the electron injection by increasing the interfacial area between the cathode and the emitting layer as reported by Carter.[28c] This is because the higher root-mean-square roughness of the Au/PF-DBMS film resulted in an in-

Table 1. Absorptions and Quantum Yields for Au NP/Polymer Nanocomposite Solid Films.

Sample	ε[a] [M^{-1} cm^{-1}]	O.D.[b] λ = 380 nm	L[c] [nm]	M[d] [mol cm^{-3}]	η[e]
PF-DBMS	4.71×10^4	0.321	102	0.768	0.57 ± 0.02
0. 5%[f] Au/PF-DBMS	4.62×10^4	0.312	90	0.750	0.73 ± 0.03
1% Au/PF-DBMS	4.68×10^4	0.324	86	0.805	0.86 ± 0.03
3% Au/PF-DBMS	4.72×10^4	0.294	79	0.788	0.80 ± 0.03
6% Au/PF-DBMS	4.70×10^4	0.292	76	0.817	0.54 ± 0.03

[a] Values of the decadic molar extinction coefficient were determined from UV-Vis spectra recorded in THF (ε = O.D./c l), where c is the concentration of the compound in solution and l is the path length of the sample.
[b] Optical density (absorbance) in the solid state.
[c] Thickness of the thin film.
[d] Concentration of the fluorescent chromophore in each composite film.
[e] Quantum yield estimated using poly[2,7-(9,9-dioctylfluorene)] (η = 0.55 ± 0.03) as the reference. See ref. [32]
[f] By weight.

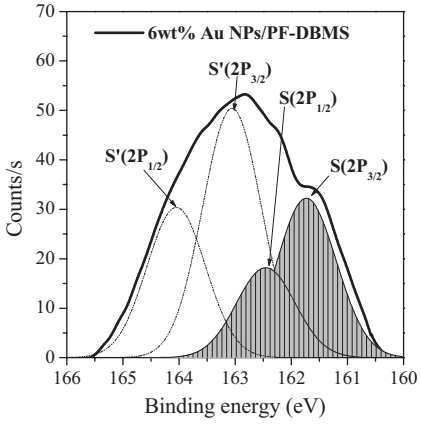

Figure 2. XPS spectra [S(2P) region] of PF-DBMS adsorbed onto Au NPs.

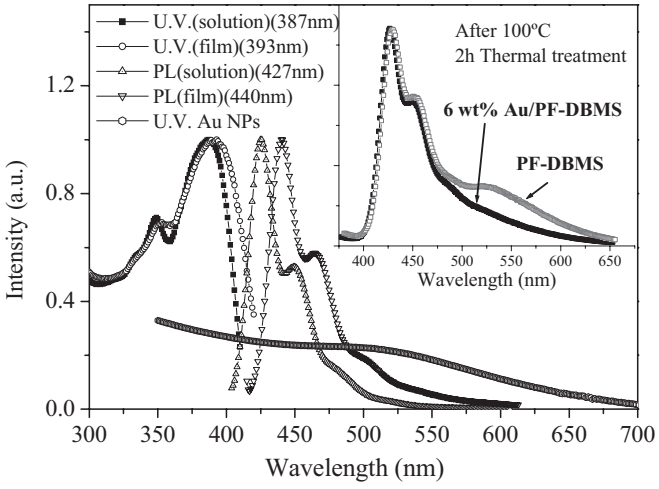

Figure 3. Normalized UV-vis absorption spectra and PL emission spectra of PF-DBMS recorded in solution (THF) and from a thin film. The inset displays the thin film after thermal treatment at 100 °C for 2 h.

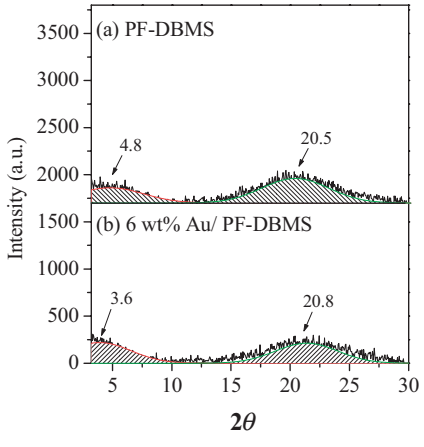

Figure 4. Deconvoluted X-ray diffraction spectra of a) PF-DBMS b) 6 wt% Au/PF-DBMS.

creased interfacial area between the film and the deposited cathode in the Au/PF-DBMS device as shown in Figure 6. When we increased the concentration of the Au NPs further (to 1 wt %), the current density of PF-DBMS decreased, but remained larger than that of pure PF-DBMS. The turn-on threshold voltage for the EL device containing 0.5 wt % Au NPs was slightly lower than that of the pristine PF-DBMS device (4.5 versus 5 V). A further increase in the Au content (to 6 wt %) led to a sudden increase in the turn-on threshold voltage to 7 V. The current density of the nanocomposite devices decreased upon increasing the number of Au NPs in excess of 1 wt %. This phenomenon can be explained by considering the balance between a mild hole trapping effect[29]—resulting from the difference in energy between the work function of the Au NPs and the highest occupied molecular orbital (HOMO) of the PEDOT:PSS layer—and enhanced electron injection. At low concentrations of Au NPs, the enhanced electron injection is more dominant than the hole trapping effect caused by the Au NPs, and, thus, the current density in the device increased. When the concentration of the Au NPs in PF-DBMS increased further, the hole trapping effect of the NPs began to dominate, resulting in a decrease in the total current density. Figure 7b displays the luminescence-voltage characteristics of the device. A greater-than-three fold increase occurred in the maximum brightness of the 1 wt % Au/PF-DBMS device, relative to that of the PF-DBMS device (1996 versus 505 Cd m^{-2}), at a drive voltage of 10 V. At the drive voltage of 10 V, the efficiency of the 1 wt % Au/PF-DBMS device is 0.6 Cd A^{-1} with a current density of 333 mA cm^{-2}. The trend in the luminescence behavior was similar to that of the current density, with the exception of the performance of the device containing 3 wt % Au NPs.

In order to verify the effect of chemical bonding of gold nanoparticles on PF-DBMS, we have carried out experiments on (i) blend of Au NPs with PF (ii) blend of Au NPs with PF-DBMS (iii) in situ synthesis Au NPs with PF-DBMS. The current density–voltage and the luminescence–voltage curves of the three cases are demonstrated in Figure 8a and b, respectively. The threshold voltage of the 1 wt % in situ synthesized Au NPs with PF-DBMS (PF-DBMS-Au) device was lower than that of the corresponding 1 wt % blend of PF-DBMS and Au NPs (PF-DBMS/Au) or blend of PF and Au NPs (PF/Au) device. The luminescence of the 1wt % PF-DBMS-Au device (1996 Cd m^{-2}) was six times and ten times as high as that of the corresponding PF/Au device (330 Cd m^{-2}) and the PF-DBMS/Au device (188 Cd m^{-2}), respectively. The lower threshold voltage and high luminescence could mainly be attributed to the efficient photo-oxidation-suppressing effect and the hole-blocking role of tethered gold nanoparticles that are much closer to the PF-DBMS molecular chains than in cases of blends. The roughness of the surface of the spin-coated sample film changed significantly, which might contribute to the enhancements to some extent. Figure 9 displays the normalized electroluminescence of the device. The EL device prepared from pure PF-DBMS emitted blue light at 425 nm and an intense green light in the range 465–650 nm. For the 6 wt % Au/PF-DBMS device, the green emission was reduced sharply, while the peak

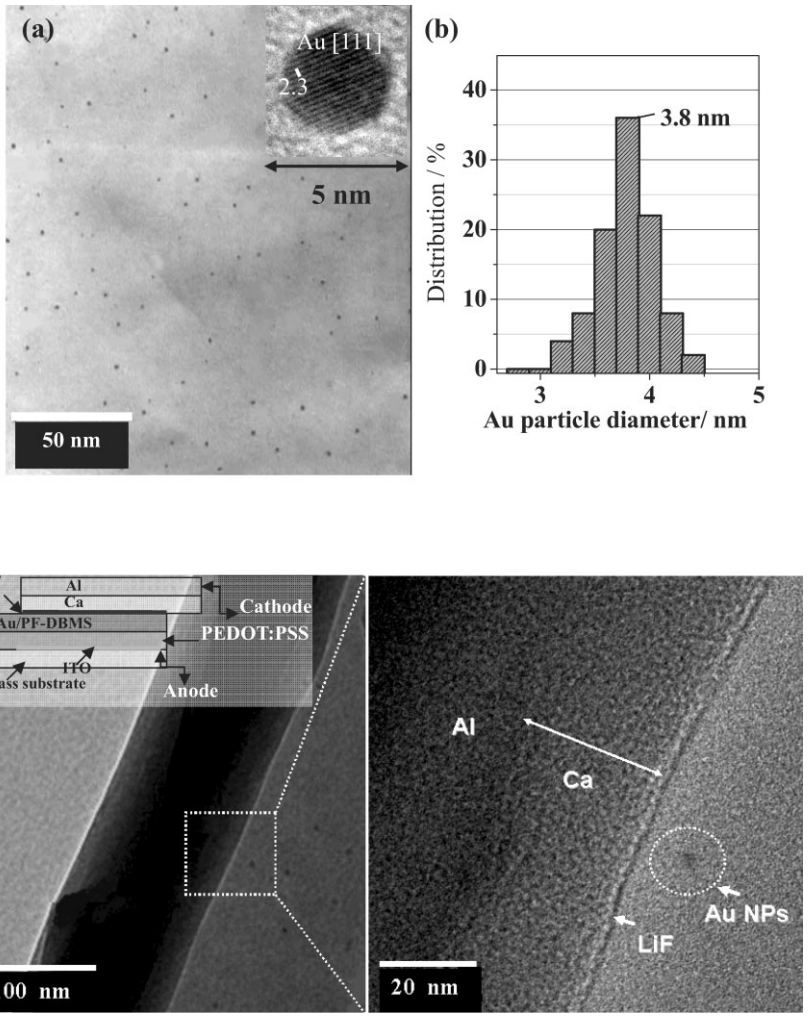

Figure 5. a) Transmission electron microscopy images of Au/PF-DBMS films. The inset displays the lattice image (lattice spacing: ca. 2.3 Å) of the Au NPs. b) Size distribution of Au NPs in the PF-DBMS polymer matrix. c) TEM images of cross-sections of the device.

at 425 nm sharpened to become the major emission signal. In addition, the full width at half maximum (FWHM) of the emission peak of the 6 wt % Au/PF-DBMS device reduced to 108 nm (from 139 nm for pure PF-DBMS), indicating that this device emitted a purer form of blue light. Compared with its PL spectrum, the changes in the relative intensities of the vibronic structure indicate that keto[33] defect was dominant during the EL process.[30,31]

3. Conclusions

In summary, we have synthesized a series of side-chain-tethered gold nanoparticles(Au NPs)/poly{2,7-(9,9′-dioctylfluorene)-*co*-4-diphenylamino-4′-bipenylmethylsulfide} (PF-DBMS) by taking advantage of in situ synthesis of gold nanoparticles through multiple $ArSCH_3$ anchor groups present on the polymer's side chains. The EL behavior of the PF-DBMS/Au NP devices indicates that they exhibit enhanced environmental stability and are suitable for use as nanocomposite emitting layers. These Au NPs/PF-DBMS nanocomposites display significantly improved device performance relative to that of the pristine PF-DBMS device. The presence of Au NPs significantly enhances the electron injection and suppresses the photooxidation of PF-DBMS.

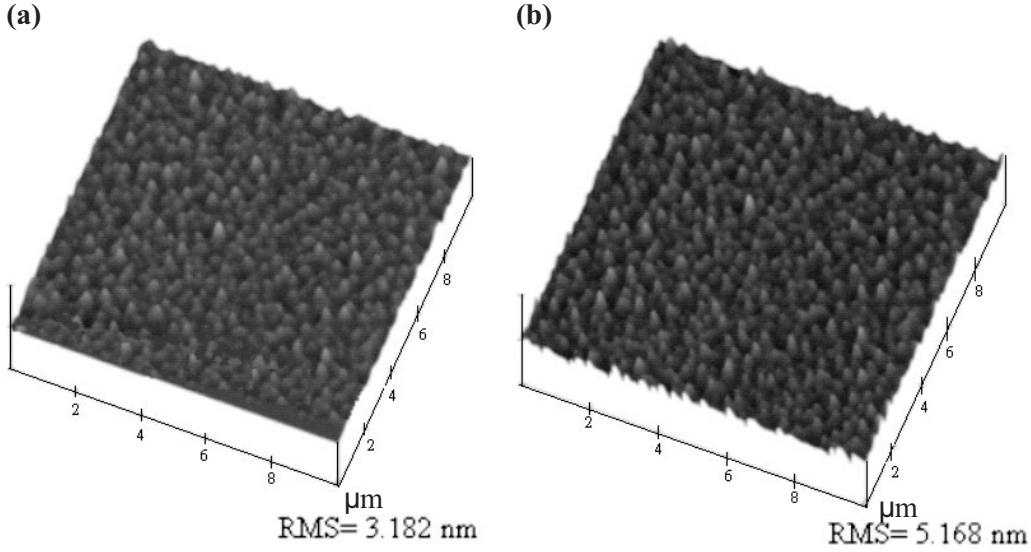

Figure 6. AFM tapping mode images of a) PF-DBMS, b) 6 wt %Au/PF- DBMS.

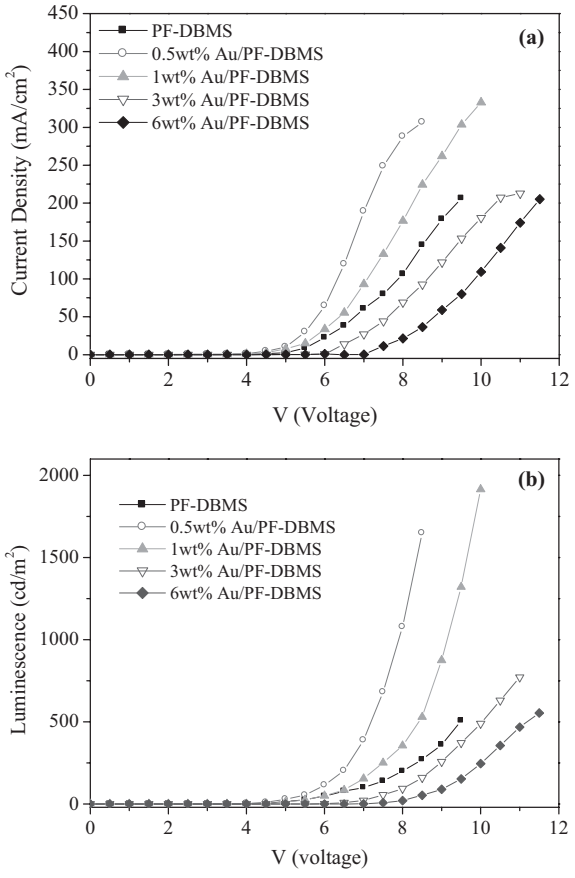

Figure 7. a) *I–V* and b) *L–V* curves of devices prepared from Au/PF-DBMS in the configuration ITO/PEDOT/polymer/LiF/Ca/Al.

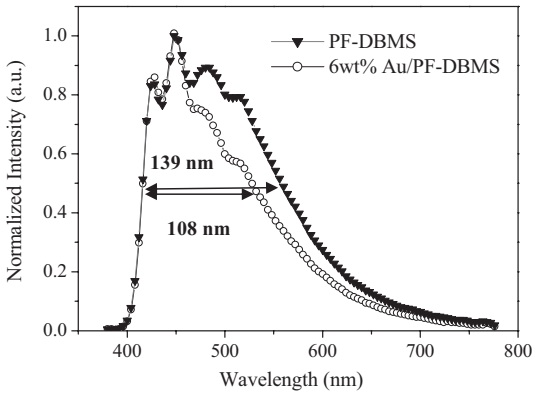

Figure 9. EL spectra of devices prepared from Au/PF-DBMS in the configuration ITO/PEDOT/polymer/LiF/Ca/Al.

4. Experimental

Synthesis of DBMS: Tris(4-bromophenyl) amine (2.58 g, 5.36 mmol) and 4-(methylthio)benzeneboronic acid (900 mg, 5.36 mmol) was stirred with Aqueous potassium carbonate (2 M) and tetrakis(triphenylphosphine)palladium (2.0 mol %) in toluene (8 mL) at 95 °C overnight. The reaction mixture was then slowly poured into water (150 mL) and extracted with chloroform (3 × 30 mL). The combined extracts were dried ($MgSO_4$), the solvents were evaporated, and the residue was purified by column chromatography (hexane/chloroform, 1:10) to afford DBMS (1.91 g, 68 %). ^{1}H NMR ($CDCl_3$): 7.52–7.41 (m, 4H), 7.34 (d, J = 9 Hz, 4H), 7.29 (d, J = 8.4 Hz, 2H), 7.08 (d, J = 8.4 Hz, 2H), 6.97 (d, J = 9 Hz, 4H), 2.50 (s, 3H) ppm. Anal. Calcd for $C_{26}H_{20}Br_2S$ (%): C, 59.56; H, 3.84. Found: C, 59.11; H, 3.51.

General Procedure for the Synthesis of Alternating Copolymers PF-DBMS: Aqueous potassium carbonate (2 M) and aliquate 336 were added to a solution of the DBMS, dibromide, and diboronate in toluene (1:4:5). The mixture was degassed and purged with nitrogen three times. The catalyst, tetrakis(triphenylphosphine)palladium (2.0 mol %), was added in one portion under a nitrogen atmosphere. The solution was then heated at 95 °C and vigorously stirred under nitrogen for 6 days. End-group capping was performed by heating the solution under reflux for 12 h sequentially with phenylboronic acid and bromobenzene. After cooling, the polymer was recovered by precipitating it into a mixture of methanol and acetone (3:1). The crude polymer was collected, purified twice by reprecipitation from THF into methanol, and subsequently dried under vacuum at 50 °C for 24 h. In this study, we have selected PF-DBMS10 (n:m = 9:1) instead of PF-DBMS30 (n:m = 7:3) as the polymer matrix to combine with Au NPs, because PF-DBMS10 has higher molecule weight, lower polydispersity (PDI), and better optical performance (in solid state).

Synthesis of Au NPs/PF-DBMS Nanocomposites: The synthesis of Au NPs was accomplished through a room-temperature, two-phase, one-pot reaction involving the reduction of $HAuCl_4$ in the presence of PF-DBMS. The $HAuCl_4$ was dissolved in H_2O and a phase-transfer reagent (tetraoctylammonium bromide) was employed to move the salt into toluene over a period of 3 h. PF-DBMS was then added to the organic solution, which was stirred for 1 h. Reduction of $AuCl_4^-$ was accomplished upon the addition of $NaBH_4$ in H_2O, which produced an immediate dark-purple-colored organic layer. The mixture was stirred for 24 h after the addition of $NaBH_4$. The dark-purple polymer/Au NP composites were precipitated into hexane, dried under vacuum at room temperature, and then redissolved for further studies. PF-DBMS was synthesized according to Scheme 1.

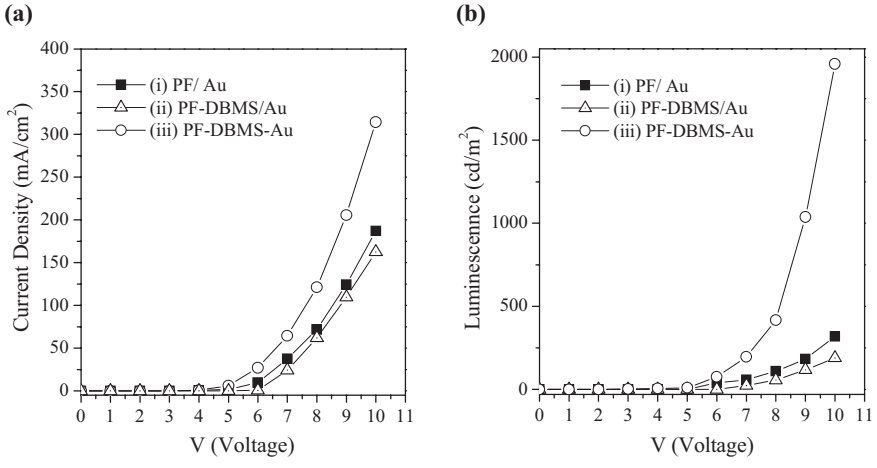

Figure 8. a) *I–V* and b) *L–V* curves of devices prepared from (i) blend of 1 wt % Au NPs with PF (ii) blend of 1 wt %Au NPs with PF-DBMS (iii) in situ synthesized 1 % Au/PF-DBMS in the configuration ITO/PEDOT/polymer/LiF/Ca/Al.

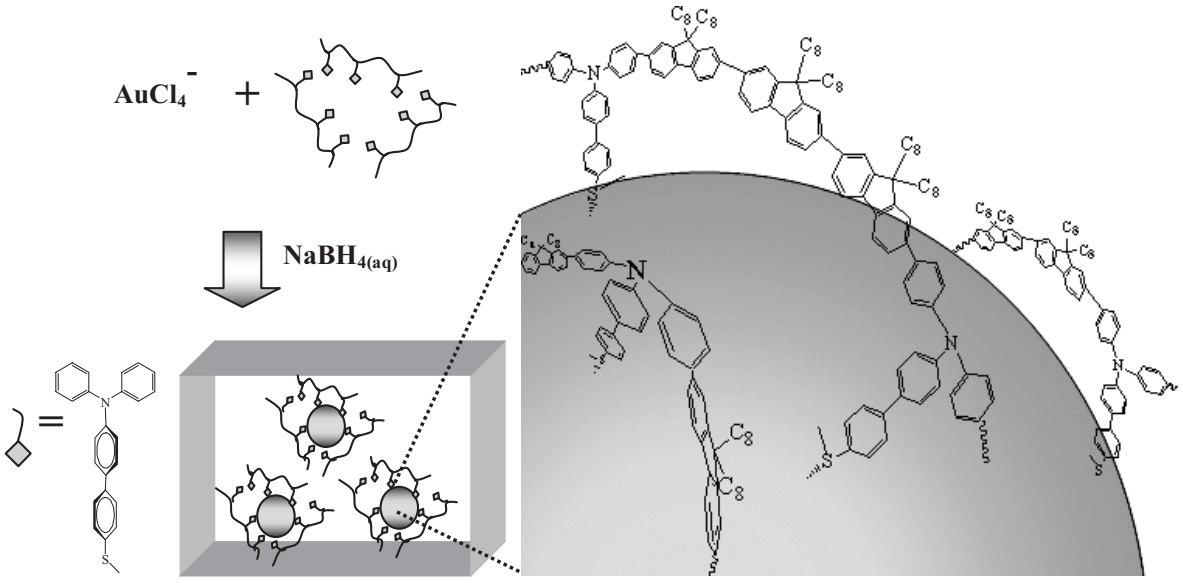

Scheme 2. A schematic drawing of the architecture of Au/ PF-DBMS nanocomposites.

Characterization: ^{1}H and ^{13}C nuclear magnetic resonance (NMR) spectra of the compounds were obtained using a Bruker DRX 300 MHz spectrometer. Mass spectra of the samples were obtained on a JEOL JMS-SX 102A spectrometer. Fourier transform infrared (FTIR) spectra of the synthesized materials were acquired using a Nicolet 360 FTIR spectrometer. Gel permeation chromatographic analyses were performed on a Waters 410 Differential Refractometer and a Waters 600 controller (Waters Styragel Column). All GPC analyses of polymers in THF solutions were performed at a flow rate of 1 mL min^{-1} at 40 °C; the samples were calibrated using polystyrene standards. UV-vis absorption and photoluminescence (PL) spectra were recorded using an HP 8453 spectrophotometer and a Hitachi F-4500 luminescence spectrometer, respectively. The diameters of the gold NPs were in the range (3.8 ± 0.3) nm, as determined using a JEOL JEM-2010 transmission electron microscope operating at 200 kV.

Device Fabrication and Testing: The electroluminescent (EL) devices were fabricated on an ITO-coated glass substrate that was precleaned and treated with oxygen plasma prior to use. A layer of poly(ethylene dioxythiophene):poly(styrene sulfonate) (PEDOT:PSS, Baytron P from Bayer Co.; ca. 40 nm thick) was formed by spin-coating from an aqueous solution (1.3 wt %). The EL layer was spin-coated—at 1500 rpm from the corresponding toluene solution (15 mg mL^{-1})—on top of the vacuum-dried PEDOT:PSS layer. The nominal thickness of the EL layer was 60 nm. Using a base pressure below 1×10^{-6} Torr, a layer of LiF (1 nm) and Ca (35 nm) was vacuum-deposited as the cathode and then a thick layer of Al was deposited as the protecting layer. The current–voltage characteristics were measured using a Hewlett-Packard 4155B semiconductor parameter analyzer. The power of the EL emission was measured using a Newport 2835-C multifunction optical meter. The brightness was calculated using the forward output power and the EL spectra of the devices; a Lambertian distribution of the EL emission was assumed.

Received: August 8, 2006
Revised: March 21, 2007
Published online: August 15, 2007

[1] A. P. Alivisatos, *Science* **1996**, *271*, 933.
[2] J. Shi, S. Gider, K. D. Babcock, D. Awschalom, *Science* **1996**, *271*, 937.
[3] a) H. Skaff, K. Sill, T. Emrick, *J. Am. Chem. Soc.* **2004**, *126*, 11 322. b) S. W. Yeh, Y. T. Chang, C. H. Chou, K. H. Wei, *Macromol. Rapid Commun.* **2005**, *25*, 1679. c) M. Krishnan, J. R. White, M. A. Fox, A. J. Bard, *J. Am. Chem. Soc.* **1983**, *105*, 7002. d) R. S. Ingram, M. J. Hostetler, R. W. Murray, *J. Am. Chem. Soc.* **1997**, *119*, 9175. e) A. C. Templeton, W. P. Wuelfing, R. W. Murray, *Acc. Chem. Res.* **2000**, *33*, 27.
[4] Y. Lin, J. Zhang, E. H. Sargent, E. Kumacheva, *J. Mater. Sci.* **2004**, *39*, 993.
[5] H. Mattoussi, L. H. Radzilowski, B. O. Dabbousi, D. E. Fogg, R. R. Schrock, E. L. Thomas, M. F. Rubner, M. G. Bawendi, *J. Appl. Phys.* **1999**, *86*, 4390.
[6] H. Zhang, C. Zhanchen, Y. Wang, K. Zhang, J. Xiulei, L. Changli, B. Yang, *Adv. Mater.* **2003**, *15*, 777.
[7] M. J. Percy, C. Barthet, J. C. Lobb, M. A. Khan, S. F. Lascelles, M. Vamvakaki, S. P. Armes, *Langmuir* **2000**, *16*, 6913.
[8] C. H. Chou, S. L. Hsu, K. Dinakaran, M. Y. Chiu, K. H. Wei, *Macromolecules* **2005**, *38*, 745.
[9] a) J. I. Lee, G. Klärner, R. D. Miller, *Chem. Mater.* **1999**, *11*, 1083. b) G. Klärner, J. I. Lee, M. H. Davey, R. D. Miller, *Adv. Mater.* **1999**, *11*, 115.
[10] a) W. L. Yu, J. Pei, W. Huang, A. J. Heeger, *Adv. Mater.* **2000**, *12*, 828. b) G. Zeng, W. L. Yu, S. J. Chua, W. Huang, *Macromolecules* **2002**, *35*, 6907.
[11] a) M. Kreyenschmidt, G. Klärner, T. Fuhrer, J. Ashenhurst, S. Karg, W. D. Chen, V. Y. Lee, J. C. Scott, R. D. Miller, *Macromolecules* **1998**, *31*, 1099. b) G. Klärner, J. I. Lee, V. Y. Lee, E. Chan, J. P. Chen, A. Nelson, D. Markiewicz, R. Siemens, J. C. Scott, R. D. Miller, *Chem. Mater.* **1999**, *11*, 1800.
[12] a) D. Marsitzky, M. Klapper, K. Mullen, *Macromolecules* **1999**, *32*, 8685. b) D. Marsitzky, J. Murray, J. C. Scott, K. R. Carter, *Chem. Mater.* **2001**, *13*, 4285. c) J. M. Lupton, P. Schouwink, P. E. Keivanidis, A. C. Grimsdale, K. Müllen, *Adv. Funct. Mater.* **2003**, *13*, 154.
[13] a) C. F. Shu, R. Dodda, F. I. Wu, M. S. Liu, A. K. Y. Jen, *Macromolecules* **2003**, *36*, 6698. b) H. J. Cho, B. J. Jung, N. S. Cho, J. Lee, H. K. Shim, *Macromolecules* **2003**, *36*, 6704. c) E. Lim, B. J. Jung, H. K. Shim, *Macromolecules* **2003**, *36*, 4288.
[14] a) E. J. W. List, R. Guentner, P. S. Freitas, U. Scherf, *Adv. Mater.* **2002**, *14*, 374. b) L. Romaner, A. Pogantsch, P. S. Freitas, U. Scherf, M. Gaal, E. Zojer, J. W. List, *Adv. Funct. Mater.* **2003**, *13*, 597. c) A. P. Kulkarni, X. Kong, S. A. Jenekhe, *J. Phys. Chem. B* **2004**, *108*, 8689.
[15] C. H. Chou, H. S. Wang, K. H. Wei, J. Y. Huang, *Adv. Funct. Mater.* **2006**, *16*, 909.

[16] J. H. Park, Y. T. Lim, O. O. Park, J. K. Kim, J. W. Yu, Y. C. Kim, *Chem. Mater.* **2004**, *16*, 688.
[17] L. A. Porter, Jr., D. Ji, S. L. Westcott, M. Graupe, R. S. Czernuszewicz, N. J. Halas, T. R. Lee, *Langmuir* **1998**, *14*, 7378.
[18] T. Yonezawa, K. Yasui, N. Kimizuka, *Langmuir* **2001**, *17*, 271.
[19] A. Manna, P.-L. Chen, H. Akiyama, T.-X. Wei, K. Tamada, W. Knoll, *Chem. Mater.* **2003**, *15*, 20.
[20] K. Torigoe, K. Esumi, *J. Phys. Chem. B* **1999**, *103*, 2862.
[21] K. Furukawa, K. Ebata, H. Nakashima, Y. Kashimura, K. Torimitsu, *Macromolecules* **2003**, *36*, 9.
[22] R. Resch, C. Baur, A. Bugacov, B. E. Koel, P. M. Echternach, A. Madhukar, N. Montoya, A. A. G. Requicha, P. Will, *J. Phys. Chem. B* **1999**, *103*, 3647.
[23] N. Felidj, J. Aubard, G. Levi, J. R. Krenn, A. Hohenau, G. Schider, A. Leitner, F. R. Aussenegg, *Appl. Phys. Lett.* **2003**, *82*, 3095.
[24] R.Balasubramanian, B. Kim, S. L. Tripp, X. Wang, M. Lieberman, A. Wei, *Langmuir* **2002**, *18*, 3676.
[25] a) X.-M. Li, M. R. de Jong, K. Inoue, S. Shinkai, J. Huskens, D. N. Reingoudt, *J. Mater. Chem.* **2001**, *11*, 1919. b) C. Zubrägel, C. Deuper, F. Schneider, M. Neumann, M. Grunze, A. Schertel, C. Wöll, *Chem. Phys. Lett.* **1995**, *238*, 308. c) Z. Li, M. Lieberman, W. Hill, *Langmuir* **2001**, *17*, 4887. d) C. R. Mayer, S. Neveu, C. Simonnet-Jégat, C. Debiemme-Chouvy, V. Cabuil, F. Secheresse, *J. Mater. Chem.* **2003**, *13*, 338.
[26] G. D. Hale, J. B. Jackson, O. E. Shmakova, T. R. Lee, N. Halas, *Appl. Phys. Lett.* **2001**, *78*, 1502.
[27] J. H. Park, Y. T. Lim, O. O. Park, Y. C. Kim, *Macromol. Rapid Commun.* **2003**, *24*, 331.
[28] a) A. P. Monkuan, H. D. Burrows, L. J. Hartwell, L. E. Horsburgh, I. Hamblett, S. Navaratnam, *Phys. Rev. Lett.* **2001**, *86*, 1358. b) S. H. Chen, A. C. Su, C. H. Su, S. A. Chen, *Macromolecules* **2005**, *38*, 379. c) S. A. Carter, J. C. Scott, P. J. Brock, *Appl. Phys. Lett.* **1997**, *71*, 1145.
[29] F. Wang, Z. J. Chen, Q. H. Gong, K. W. Wu, X. S. Wang, B. W. Zhang, F. Q. Tang, *Appl. Phys. Lett.* **1999**, *75*, 3243.
[30] T. Q. Nguyen, I. B. Martini, J. Liu, B. J. Schwartz, *J. Phys. Chem. B* **2000**, *104*, 237.
[31] a) S. H. Chen, A. C. Su, Y. F. Huang, C. H. Su, G. Y. Peng, S. A. Chen, *Macromolecules* **2002**, *35*, 4229. b) L. O. Brown, J. E. Hutchison, *J. Phys. Chem. B* **2001**, *105*, 8911.
[32] a) R. G. Dondon, V. P. Khilya, A. D. Roshal, S. Fery-Forgues, *New J. Chem.* **1999**, *23*, 923. b) A. W. Grice, D. D. C. Bredley, M. T. Bernius, M. Inbasekaran, W. W. Wu, E. P. Woo, *Appl. Phys. Lett.* **1998**, *73*, 629.
[33] a) C. L. Chochos, J. K. Kallitsis, V. G. Gregoriou, *J. Phys. Chem. B* **2005**, *109*, 8755. b) S. Qiu, P. Lu, X. Liu, F. Shen, L. Liu, Y. Ma, J. Shen, *Macromolecules* **2003**, *36*, 9823. c) L. Yang, J.-K. Feng, A.-M. Ren, *J. Org. Chem.* **2005**, *70*, 5987.